Appl. Phys. A 81, 561–564 (2005)
DOI: 10.1007/s00339-004-2673-3

Applied Physics A
Materials Science & Processing

V.R. REDDY[1]
S.-H. KIM[2]
T.-Y. SEONG[2,✉]

Formation of thermally stable low-resistance Ti/W/Au ohmic contacts on *n*-type GaN

[1] Department of Electronics, University of Mysore, Post-Graduate Centre, Hemagangotri, Hassan – 573 220, India
[2] Department of Materials Science and Engineering, Kwangju Institute of Science and Technology, 1 Oryong-dong, Puk-gu, Gwangju 500-712, Korea

Received: 29 September 2003/Accepted: 4 February 2004
Published online: 16 April 2004 •

ABSTRACT A Ti(12 nm)/W(20 nm)/Au(50 nm) metallization scheme has been investigated for obtaining thermally stable low-resistance ohmic contacts to *n*-type GaN (4.0×10^{18} cm^{-3}). It is shown that the current–voltage (*I*–*V*) characteristics of the samples are abnormally dependent on the annealing temperature. For example, the samples that were annealed at temperatures below 750 °C for 1 min in a N_2 ambient show rectifying behavior. However, annealing the samples at temperatures in excess of 850 °C results in linear *I*–*V* characteristics. The contact produces a specific contact resistance as low as 8.4×10^{-6} Ω cm^2 when annealed at 900 °C. It is further shown that the contacts are fairly thermally stable even after annealing at 900 °C; annealing the samples at 900 °C for 30 min causes insignificant degradation of the electrical and structural properties. Based on glancing angle X-ray diffraction and Auger electron microscopy results, the abnormal temperature dependence of the ohmic behavior is described and discussed.

PACS 72.80.Ey; 73.40.Cg; 73.20.At; 79.60Bm; 73.40.Gk

1 Introduction

Gallium nitride (GaN) is one of the most promising materials for the fabrication of efficient blue light sources [1, 2], high-power microwave devices [3] and high-temperature electronic devices [4]. One of the key requirements for these devices is the formation of low resistance and reliable ohmic contacts, which are capable of withstanding elevated temperatures. However, forming low resistance and thermally stable ohmic contacts to GaN-related semiconductors is still a challenge.

Over the past few years, attempts have been made to obtain low-resistance ohmic contacts to *n*-GaN [5–7]. Foressi and Moustakas [5] first used Al or Au schemes for the formation of ohmic contacts to *n*-GaN and showed that each scheme was ohmic with a specific contact resistance of $\sim 10^{-3}$ Ω cm^2, when annealed at 575 °C. To improve the ohmic properties of Au and Al contacts to *n*-GaN, bilayer schemes, such as Ti/Al and Ti/Au, were employed. For example, Lin et al. [7] reported that Ti/Al contacts produced a specific contact resistance of $\sim 10^{-6}$ Ω cm^2 upon annealing at 900 °C for 30 s in a N_2 ambient. The formation of a TiN interfacial layer was suggested to be important for the achievement of good ohmic contacts [7]. Later on, Kwak et al. [8] showed that the Ti/Al contacts to Ga-face *n*-GaN yielded a specific contact resistance of 2×10^{-5} Ω cm^2 after annealing at temperatures higher than 600 °C for 30 s in a N_2 ambient. Papanocolau et al. [9], investigating Ti/Al and Cr/Al contacts to *n*-GaN, reported that the contact schemes were ohmic with contact resistivities of 1×10^{-5} and 3.8×10^{-5} Ω cm^2 after vacuum-annealing at 1100 and 700 °C, respectively. Ti/Al-based ohmic contacts have been widely used as an *n*-type ohmic electrode for light emitting diodes [7–10]. However, aluminum (Al) is vulnerable to oxidation at elevated temperatures. Therefore, in this work we have investigated an Al-free scheme of Ti/W/Au for the formation of low resistance ohmic contacts to *n*-GaN (4.0×10^{18} cm^{-3}). Tungsten (W) was selected as a middle layer because of its refractory nature and reactivity with GaN, as demonstrated by Cole et al. [11] and Zeitouny et al. [12]. It is shown that the Ti/W/Au contacts yield a specific contact resistance as low as 8.4×10^{-6} Ω cm^2 upon annealing at 900 °C for 1 min in a N_2 ambient.

2 Experimental details

An undoped GaN layer with a thickness of 2 μm was grown on a c-plane sapphire substrate by metalorganic chemical vapor deposition. This was followed by the growth of 2 μm *n*-type GaN doped with Si. The carrier concentration was determined to be 4.07×10^{18} cm^{-3} by means of Hall effect measurements with the Van der Pauw geometry. Before metallization, the *n*-GaN layer was ultrasonically degreased with warm trichloroethylene, acetone and methanol for 5 min in each. It was then dipped into a buffered oxide etch (BOE) solution for 10 min to remove surface oxide and rinsed in DI water. CTLM patterns were then defined on the surface treated *n*-GaN layer by a standard photolithography technique. The outer dot radius was 75 μm and the spacing between the inner and outer radii was varied from 4–24 μm. Prior to metal deposition, the patterned layer was dipped in a BOE solution for 30 s, blown dry with N_2 gas, and immediately loaded into an electron beam evaporation system. A Ti/W/Au (12 nm/20 nm/50 nm) film was then deposited on the surface treated *n*-GaN. Some of the samples were rapid thermal annealed at temperatures ranging from

✉ Fax: +82-62/970-2304, E-mail: tyseong@kjist.ac.kr

400–900 °C for 1 min in a N_2 ambient. Current–voltage (I–V) characteristics were measured using a semiconductor parameter analyzer (HP4155A). Auger depth profiling (AES: a PHI 670 Auger microscope) was carried out to observe the extent of interdiffusion between the metal layers and the n-GaN. Glancing angle X-ray diffraction (GXRD) (using Cu K_α radiation) (a Rigaku diffractometer: D/MAX-RC) was employed to identify the interfacial phases formed upon annealing.

3 Results and discussion

Figure 1 shows the typical I–V characteristics of Ti/W/Au ohmic contacts on n-GaN as a function of the annealing temperature, measured between the ohmic pads with a spacing of 4 μm. The as-deposited sample shows non-linear I–V characteristics. It is, however, noted that annealing the sample at 500 °C results in a rectifying characteristic. After annealing at 750 °C, the I–V behavior becomes somewhat improved, although still rectifying. However, the samples exhibit linear I–V characteristics at temperatures in excess of 850 and 900 °C. Similar abnormal temperature dependence of ohmic behavior was also reported in Ti/Al-based schemes by Papanicoaou et al. [13] and Kumar et al. [14] who attributed such behavior to the formation of a heterojunction or a quasi-metal-insulator-semiconductor structure. However, the exact mechanism for the abnormal ohmic behaviour remains to be found. Specific contact resistance was determined from plots of the measured total resistance versus the spacings between the CTLM pads [15]. The least square curve-fitting method was used to fit a straight line to the experimental data. Specific contact resistance was measured to be $8.4 \times 10^{-6}\ \Omega\,\mathrm{cm}^2$ for the sample annealed at 900 °C.

Figure 2 shows the AES depth profiles of the Ti/W/Au contacts on n-GaN before and after annealing. For the as-deposited sample, Fig. 2a, the individual layers of Ti, W and Au are well-defined, indicating no significant interdiffusion between the metal films and the n-GaN. For the 550 °C-annealed sample, Fig. 2b, some amount of N was outdiffused into the Ti layer, indicating the possibility of the formation of an initial phase of TiN at the Ti/GaN interface. For the 900 °C sample, Fig. 2c, a large amount of nitrogen outdiffused into

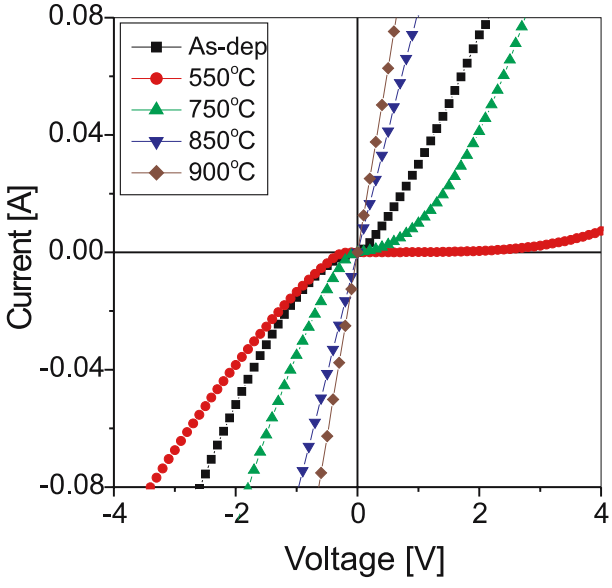

FIGURE 1 The typical I–V characteristics of Ti/W/Au ohmic contacts on n-GaN as a function of the annealing temperature, measured between the ohmic pads with a spacing of 4 μm

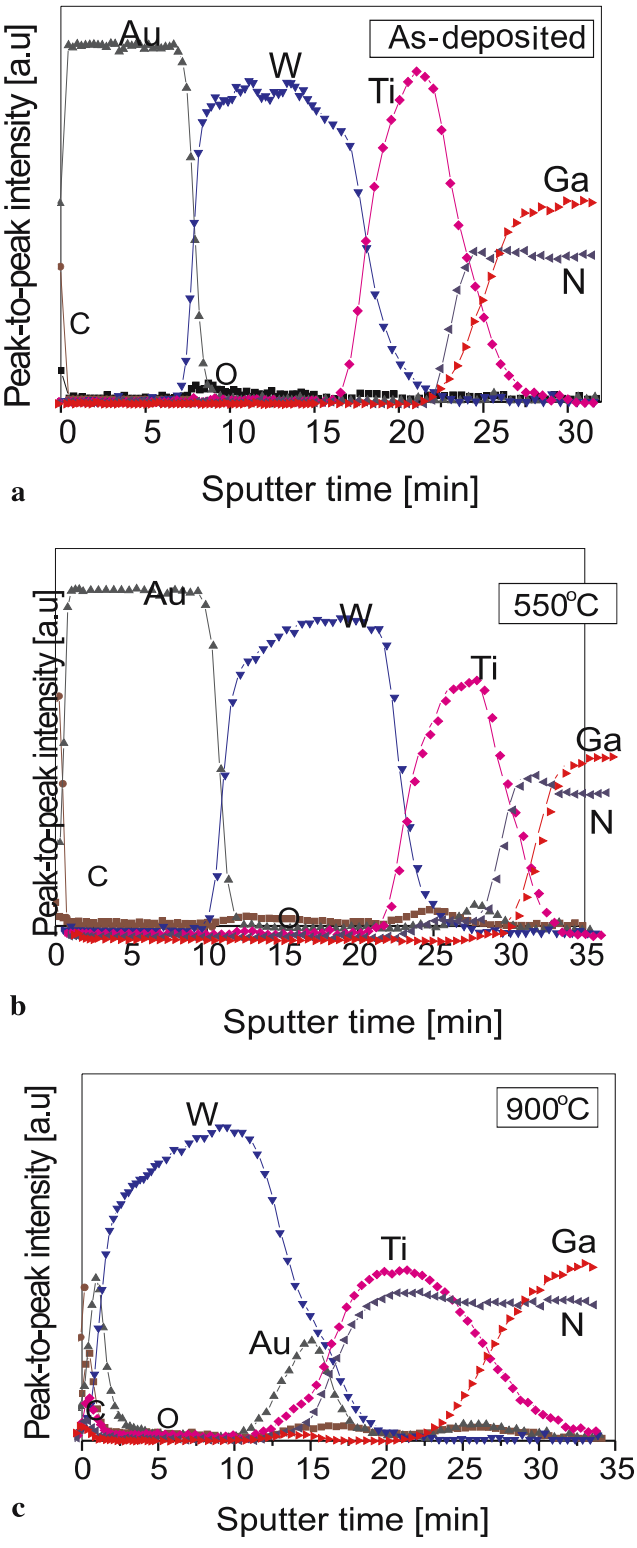

FIGURE 2 The AES depth profiles of the Ti/W/Au ohmic contacts to n-GaN before and after annealing: **a** as-deposited; **b** annealed at 550 °C; **c** 900 °C

the metal layers. Furthermore, some amount of Au diffused to the W/Ti interface region through the W layer, where a small amount of Ga was also detected. This indicates that Ti-N, W-N and Au-Ga reaction products were formed during the annealing process, as will be confirmed by GXRD examination.

Figure 3 shows GXRD plots obtained from the Ti/W/Au contacts after annealing at temperatures of 550 and 900 °C. For the sample annealed at 550 °C, Fig. 3a, the GXRD plot reveals the characteristic diffraction peaks of Ti, W and Au. In addition, there is a broad weak peak, which is identified as initial Ti_4N_{3-x} phase, as expected from the AES result (Fig. 2b). For the 900 °C sample, Fig. 3b, in addition to the W and Au diffraction peaks, there are extra peaks, which is indicative of the formation of new interfacial phases. These phases are identified as Ti_3N_{2-x}, Ti_4N_{3-x}, W_2N, WN and $GaAu_2$. It is noted that gallide phase was also formed, even though the nitride phases were dominant. This is in good agreement with the AES result, Fig. 2c.

The surface morphology of the Ti/W/Au contacts before and after annealing was characterized using atomic force microscopy (AFM). The AFM images (not shown) indicate that the surface morphology of the as deposited sample is reasonably smooth with a root-mean-square (RMS) roughness of 3.0 nm. When annealed at 900 °C, the sample surface was not significantly degraded; the RMS roughness was 3.8 nm.

To ensure the suitability of the Ti/W/Au scheme for high temperature and high power applications, the contact was subjected to annealing treatment. Figure 4 shows the variation of the specific contact resistance of the Ti/W/Au contacts as a function of annealing time at 900 °C. As the annealing time increased, the specific contact resistance changed only very slightly, increasing from $8.4 \times 10^{-6}\ \Omega\,cm^2$ for 1 min to $1.6 \times 10^{-5}\ \Omega\,cm^2$ for 30 min. This finding, together with the AFM results, shows that the Ti/W/Au scheme does not seriously suffer from thermal degradation during annealing, even at 900 °C.

The electrical properties of the Ti/W/Au contacts were heavily dependent on the annealing temperatures. For example, the samples annealed below 750 °C revealed poorer electrical properties compared with the as-deposited sample. The first degradation of the ohmic behavior might be attributed to the formation of a heterojunction or a quasi-metal-insulator-semiconductor structure, resulting in a higher barrier height [13, 14], although the precise mechanism is not clear at this moment. Then the electrical properties were improved significantly after annealing at temperatures in excess of 850 °C. This improved annealing temperature dependence could be explained as follows. First, the improvement of the contact resistivity could be associated with the formation of particular types of interfacial phases, such as Ti-N and W-N, as shown by the GXRD results (Fig. 3). The AES and GXRD results showed that although a small fraction of gallide phase was observed, the interfacial nitride phases were predominantly formed in the annealed samples. The formation of the nitrides phases results in the generation of nitrogen vacancies near the GaN surface region, which plays an important role in reducing contact resistivity. According to Jenkins and Dow, nitrogen vacancies in GaN act as donors [16]. On the

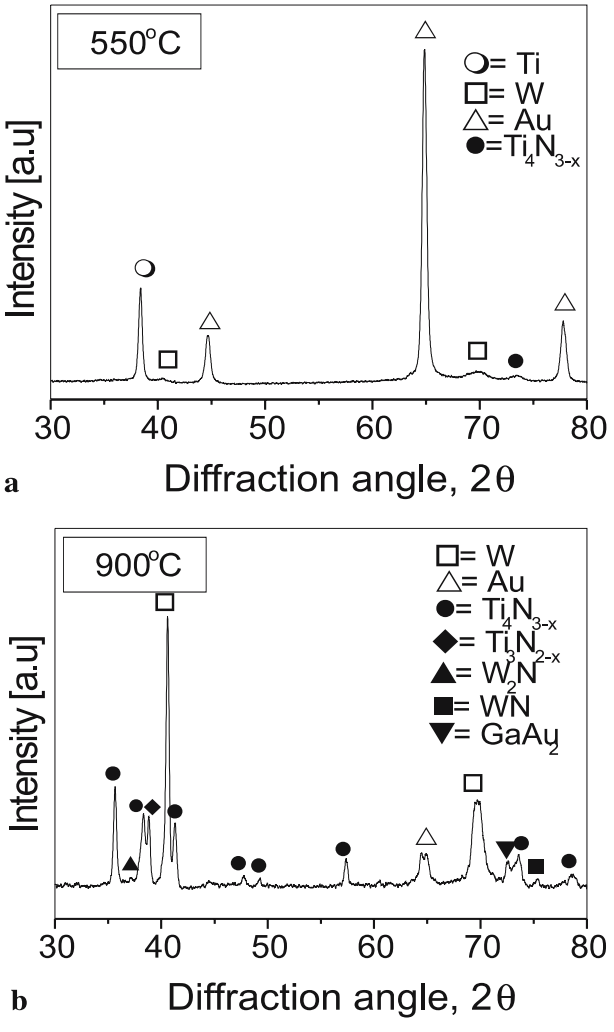

FIGURE 3 Glancing angle XRD plots obtained from the Ti/W/Au contacts annealed at **a** 550 °C and **b** 900 °C

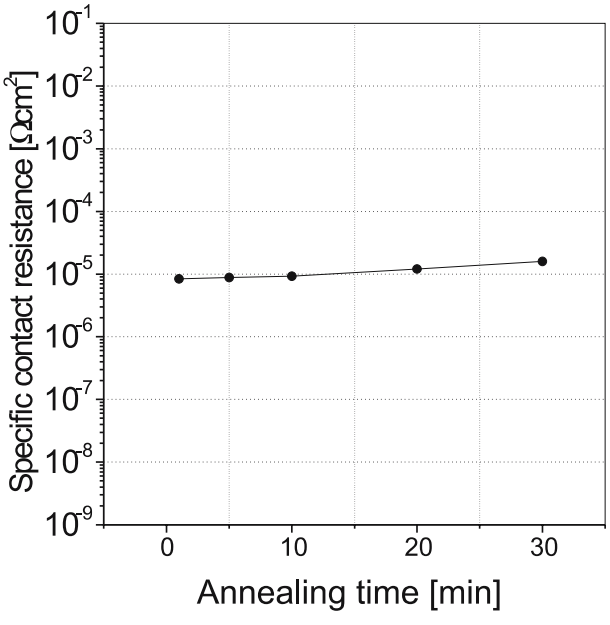

FIGURE 4 The annealing time dependence of the specific contact resistance of the Ti/W/Au contacts at 900 °C

other hand, the formation of the gallide phase results in Ga vacancies, which were known to act as deep acceptors [17]. However, nitrogen vacancies are predominant over Ga vacancies, as shown by the results of AES and XRD, Figs. 2c and 3c. Therefore, the increase in carrier concentration at the GaN surface region, leading to a reduction of the surface-barrier height to *n*-GaN, could be responsible for the significant reduction in the contact resistivity of the Ti/W/Au contacts annealed at temperatures higher than 850 °C. This finding is consistent with the results previously observed by Luther et al. [18] and Dimitriadis et al. [19]. Luther et al. [18], studying Ti-based contacts to *n*-GaN, showed that the formation of the TiN_x interfacial phase, resulting in the generation of nitrogen vacancies, is necessary for ohmic contact formation. Another possibility may be related to an increase in contact area between the metallization schemes and the GaN due to the interfacial reactions during thermal annealing [20, 21].

4 Conclusion

We achieved low specific contact resistance for moderately doped *n*-type GaN ($4.0 \times 10^{18}\,\mathrm{cm}^{-3}$) using the Ti/W/Au scheme. It was shown that the *I*–*V* characteristics of the contacts became degraded upon annealing at temperatures below 750 °C for 1 min in a N_2 ambient compared with that of the as-deposited sample. However, it was improved drastically when annealed at temperatures above 850 °C. Measurements showed that the contact annealed at 900 °C produces a low specific contact resistance of $8.4 \times 10^{-6}\,\Omega\,\mathrm{cm}^2$. Based on the AES and XRD results, the first degraded *I*–*V* behavior was attributed to the formation of the initial TiN phase, leading to the formation of a heterojunction or a quasi-metal-insulator-semiconductor structure. On the other hand, the improved ohmic behavior at elevated temperature was ascribed to the reduction of the surface-barrier height to *n*-GaN due to the formation of Ti-N and W-N interfacial phases. It was further shown that the prolonged annealing treatment at 900 °C does not cause significant degradation in the electrical and thermal properties of the Ti/W/Au contacts. This result indicates that the Ti/W/Au contact may be a good choice for high temperature device applications.

ACKNOWLEDGEMENTS This work was supported in part by grant No. (R01-2002-000-00356-0) from the Basic Research Program of the Korea Science & Engineering Foundation.

REFERENCES

1 S. Nakamura, T. Mukai, S. Senoh: Jpn. J. Appl. Phys. **30**, L1998 (1991)
2 H. Amano, M. Kito, X. Hiramatsu, I. Akasaki: Jpn. J. Appl. Phys. **28**, L2112 (1998)
3 H. Morkoc, S. Strite, G.B. Gao, M.E. Lin, B. Serdlov, M. Burns: J. Appl. Phys. **76**, 1363 (1994)
4 M.A. Khan, M.S. Shur, Q. Chen: Appl. Phys. Lett. **68**, 3022 (1996)
5 J.S. Foresi, T.D. Moustakas: Appl. Phys. Lett. **62**, 2859 (1993)
6 M.E. Lin, F.Y. Hung, H. Morkoc: Appl. Phys. Lett. **64**, 2557 (1994)
7 M.E. Lin, C. Ma, F.Y. Huang, Z.F. Fan, L.H. Allen, H. Morkoc: Appl. Phys. Lett. **64**, 1003 (1994)
8 J.S. Kwak, K.Y. Lee, J.Y. Han, J. Cho, O.H. Nam, Y. Pak: Appl. Phys. Lett. **79**, 3254 (2001)
9 N.A. Papanocolaou, K. Zekentes: Solid-State Electron. **46**, 1975 (2002)
10 B.P. Luther, S.E. Mohney, T.N. Jackson, M.A. Khan, Q. Chen, J.W. Yang: Appl. Phys. Lett. **70**, 57 (1997)
11 M.W. Cole, D.W. Eckart, W.Y. Han, R.L. Pfeffer, T. Monahan, F. Ren, C. Yuan, R.A. Stall, S.J. Pearton, Y. Li, Y. Lu: J. Appl. Phys. **80**, 278 (1996)
12 A. Zeitouny, M. Eizenberg, S.J. Pearton, F. Ren: Mater. Sci. Eng. B **59**, 358 (1999)
13 N.A. Papanicolaou, M.V. Rao, J. Mittereder, W.T. Anderson: J. Vac. Sci. Technol. B **19**, 261 (2001)
14 V. Kumar, L. Zhou, D. Selvanathan, I. Adesida: J. Appl. Phys. **92**, 1712 (2002)
15 G.S. Marlow, M.B. Das: Solid-State Electron. **25**, 91 (1982)
16 D.W. Jenkins, J.D. Dow: Phys. Rev. B **39**, 3317 (1989)
17 J. Sun, K.A. Rickert, J.M. Redwing, A.B. Ellis, F.J. Himpsel, T.F. Kuech: Appl. Phys. Lett. **76**, 415 (2000)
18 B.P. Luther, S.E. Mohney, T.N. Jackson: Semicond. Sci. Technol. **13**, 1322 (1998)
19 C.A. Dimitriadis, T. Karakostas, S. Logothetidis, G. Kamarinos, J. Brini, G. Nouet: Solid-State Electron. **43**, 1969 (1999)
20 J.O. Song, S.-H. Kim, J.S. Kwak, T.-Y. Seong: Appl. Phys. Lett. **83**, 1154 (2003)
21 H.-K. Kim, S.H. Han, T.-Y. Seong, W.K. Choi: Appl. Phys. Lett. **77**, 1647 (2000)